Ocean acidification increases iodine accumulation in kelp-based coastal food webs

Xu, Dong; Brennan, Georgina; Xu, Le; Zhang, Xiao W.; Fan, Xiao; Han, Wen T.; Mock, Thomas; McMinn, Andrew; Hutchins, David A.; Ye, Naihao

Global Change Biology

DOI:
10.1111/gcb.14467

Published: 01/02/2019

Peer reviewed version

Ocean acidification increases iodine accumulation in kelp-based coastal food webs

Running head: Ocean acidification increases iodine in kelp

Dong Xu[1,2,#], Georgina Brennan[3,#], Le Xu[1], Xiao W. Zhang[1], Xiao Fan[1], Wen T. Han[1], Thomas Mock[4], Andrew McMinn[5,6], David A. Hutchins[7], Naihao Ye[1,2,*]

[1]Yellow Sea Fisheries Research Institute, Chinese Academy of Fishery Sciences, Qingdao, China

[2]Function Laboratory for Marine Fisheries Science and Food Production Processes, Qingdao National Laboratory for Marine Science and Technology, Qingdao, China

[3]Molecular Ecology and Fisheries Genetics Laboratory, School of Biological Sciences, Bangor University, Bangor LL57 2UW, UK

[4]School of Environmental Sciences, University of East Anglia, Norwich Research Park, Norwich, United Kingdom

[5]Institute for Marine and Antarctic Studies, University of Tasmania, Hobart, Tasmania, Australia

[6]Fisheries College, Ocean University of China, Qingdao, China

[7]Department of Biological Sciences, University of Southern California, Los Angeles, CA, USA

[#]These authors contributed equally to this work.

Correspondence: Naihao Ye, tel. 86-532-85830360, fax 86-532-85830360, e-mail: yenh@ysfri.ac.cn.

Keywords: Ocean acidification, iodine metabolism, *Saccharina japonica*, kelp,

vanadium-dependent haloperoxidase, thyroid hormone

Paper type: Primary Research Article

Accepted for Publication in Global Change Biology (19th Sept 2018).

ABSTRACT

Kelp are main iodine accumulators in the ocean, and their growth and photosynthesis are likely to benefit from elevated seawater CO_2 levels due to ocean acidification. However, there are currently no data on the effects of ocean acidification on iodine metabolism in kelp. As key primary producers in coastal ecosystems worldwide, any change in their iodine metabolism caused by climate change will potentially have important consequences for global geochemical cycles of iodine, including iodine levels of coastal food webs that underpin the nutrition of billions of humans around the world. Here, we found that elevated pCO_2 enhanced growth and increased iodine accumulation not only in the model kelp *Saccharina japonica* using both short-term laboratory experiment and long-term *in situ* mesocosms, but also in several other edible and ecologically significant seaweeds using long-term *in situ* mesocosms. Transcriptomic and proteomic analysis of *Saccharina japonica* revealed that most vanadium-dependent haloperoxidase genes involved in iodine efflux during oxidative stress are down-regulated under increasing pCO_2, suggesting that ocean acidification alleviates oxidative stress in kelp, which might contribute to their enhanced growth. When consumed by abalone (*Haliotis discus),* elevated iodine concentrations in *S. japonica* caused increased iodine accumulation in abalone, accompanied by reduced synthesis of thyroid hormones. Thus, our results suggest that kelp will benefit from ocean acidification by a reduction in environmental stress however, iodine levels in kelp-based coastal food webs will increase, with potential impacts on biogeochemical

67 cycles of iodine in coastal ecosystems.

68

69 **INTRODUCTION**

70 Anthropogenic emissions of CO_2, associated ocean acidification (OA) and global
71 warming, are increasing at rates unprecedented in the geological record (Sunday et al.,
72 2017; Thomsen et al., 2017). These changes are expected to directly affect primary
73 producers by changing growth rates, photosynthesis and metabolism, and indirectly by
74 reducing biodiversity and altering ecosystem structure (Enochs et al., 2015; Martínez-
75 Botí et al., 2015; Myers et al., 2017; Ullah, Nagelkerken, Goldenberg, & Fordham,
76 2018). Furthermore, OA is predicted to cause an increase in the accumulation of toxic
77 phenolic compounds across multiple trophic levels, from phytoplankton to zooplankton
78 (Jin et al., 2015). Higher temperatures are also expected to increase the concentrations
79 of nutrients such as nitrogen (N), potassium (K), and magnesium (Mg) stored in living
80 biomass (Zhang et al., 2018) and impact the global biotic metabolic rates (Dillon, Wang,
81 & Huey, 2010). Metabolic rate changes and nutrient variation under climate change will
82 affect human health through consumption of these organisms (Jin et al., 2015;
83 McKibben et al., 2017; Zhu et al., 2018) and potentially impact food security (Bloom,
84 Burger, Asensio, & Cousins, 2010; Loladze, 2002; Myers et al., 2017; Phalkey, Aranda-
85 Jan, Marx, Höfle, & Sauerborn, 2015). However, climate impacts on the nutrient
86 composition of primary producers (such as, seaweeds) in coastal ecosystem has, to date,
87 been little explored.

88

89 Seaweeds, including, brown, red, and green algae are a rich source of iodine (Küpper,
90 2015; Küpper et al., 2008; Nitschke & Stengel, 2015; Ye et al., 2015) and are widely
91 harvested for food and exploited for commercial alginate and iodine. Iodine is an
92 essential nutrient required for the synthesis of thyroid hormones (THs),
93 triiodothyronine (T3) and thyroxine (T4) (Berg et al., 2017). Iodine deficiency in
94 humans can result in unexpected health problems such as hypothyroidism and goiter,
95 whereas high iodine intake from seaweeds can lead to hyperthyroidism, a reversible
96 condition which can cause symptoms such as nontoxic or diffuse nodular goiter, latent
97 Graves' disease and long standing iodine deficiency (Leung & Braverman, 2014).
98 Natural consumers of seaweeds such as fish and shellfish are also a rich dietary source
99 of iodine for humans (Nitschke & Stengel, 2015). It is therefore essential to understand
100 how the iodine content of seafood will change under global climate change. This
101 information can for instance be used by the World Health Organization (WHO) to
102 provide recommendations on appropriate levels of seaweeds consumption to maintain
103 a sufficient daily iodine intake (Fig. 1).
104
105 With respect to iodine, kelp (order Laminariales) are particularly important as they are
106 not only being the greatest iodine accumulators among living organisms, but also
107 playing an important role in the global biogeochemical cycle of iodine (Küpper, 2015;
108 Küpper et al., 2008). In *Laminaria* tissue, iodine is mostly stored as iodide on the thallus
109 surface and in the apoplast. Iodide efflux occurs under oxidative stress and iodide in the
110 peripheral tissues acts as an inorganic antioxidant to detoxify both aqueous oxidants

and ozone, stimulating the release of molecular iodine and volatile iodinated compounds to the atmosphere (Cosse et al., 2009; Küpper & Kroneck, 2014). Oxidative burst and associated iodine metabolism also play a direct defensive role in both controlling the growth of potentially pathogenic bacteria living at the thallus surface and scavenging a variety of reactive oxygen species (ROS) (Küpper et al., 2008; Küpper, Müller, Peters, Kloareg, & Potin, 2002; Strittmatter et al., 2016). During oxidative burst, algal cells rapidly release large amounts of activated oxygen species (AOS), such as superoxide (O_2^-), hydrogen peroxide (H_2O_2) or hydroxyl radicals (OH^-). This release is elicited by exposure to oligomeric degradation products of alginate and possibly other molecular signals. It has been suggested that the mechanism of iodine antioxidation is linked to the production of vanadium-dependent haloperoxidases (vHPOs), which comprises seventeen vanadium-dependent bromoperoxidases (vBPOs) and fifty-nine iodoperoxidases (vIPOs) in the *S. japonica* genome (Butler & Carter-Franklin, 2004; Cosse et al., 2009; Ye et al., 2015) (Fig. 1).

Despite widespread interest in the biological response of kelp to climate change, there is currently no information on the *in situ* molecular response associated with iodine metabolism. Here, three ecologically and socio-economically important kelp species (*S. japonica*, *U. pinnatifida*, and *M. pyrifera*), as well as another four coastal seaweeds (*Ulva pertusa* and *Ulva intestinalis* in Chlorophyta; *Gracilaria lemaneiformis* and *Gracilaria chouae* in Rhodophyta) were used to study the effect of increasing pCO_2 on iodine accumulation of seaweeds using both short-term laboratory experiments and one

long-term, *in situ* experiment. In a feeding experiment, the transfer of iodine between *S. japonica* and its consumer *Haliotis discus* was investigated. We used these experiments to explore: (i) the effect of elevated pCO_2 on iodine accumulation in kelp-based coastal food webs; (ii) whether short-term laboratory experiments can be compared with *in situ* ocean mesocosms; (iii) the molecular mechanism involved in iodine metabolism at the transcriptional and protein level in response to elevated pCO_2. Together, the research presented here will be used to assess the global biogeochemical cycle of iodine under future climate change and provide information for making recommendations on appropriate levels of seaweeds consumption to reach adequate daily iodine intake.

MATERIALS AND METHODS

Algal material and culture conditions

For the laboratory experiments, young sporophytes of *S. japonica* were collected from semi-enclosed Sungo Bay, located on the northwestern coast of the Yellow Sea, China (37°01′–37°09′ N, 122°24′–122°35′ E) in December 2016, when the mean seawater temperature was 10.3°C. Similar sized algal samples (average length is 10 cm) were transported back to the laboratory within three hours, in a tank of cold seawater. In the laboratory, the intact samples were washed with sterile seawater until they were free from visible epiphytes and then pre-cultured in aquaria supplemented with f/2 medium (Guillard, 1975) at 10 ± 1°C with vigorous air bubbling for 2 days before the start of the experiment. The lighting conditions were set at 100 μmol photons m^{-2} s^{-1} supplied

155 by white fluorescent lamps, with a photoperiod of 12 h light and 12 h darkness.

156

157 **Effect of increasing pCO_2 and temperature on iodine accumulation**

158 To study the individual effect of temperature on iodine accumulation in *S. japonica*
159 sporophytes, a gradient of five temperatures (5°C, 10°C, 15°C, 20°C, and 23°C) was
160 established, mimicking the annual variation of temperature during the growth period.
161 To examine the combined effect of increasing pCO_2 and temperature, three
162 temperatures (10°C, 15°C, 20°C) and five pCO_2 levels (400 μatm, 700 μatm, 1,000
163 μatm, 1,500 μatm, and 2,000 μatm), were selected (Table S1). These pCO_2 levels were
164 chosen as they reflect current and future pCO_2 levels up to the year 2,300 under IPCC
165 (Intergovernmental Panel on Climate Change) scenario RCP 8.5. The experiment was
166 conducted in flasks using three biological replicates per treatment. Before experiments,
167 algal samples were pre-cultured in seawater under various pCO_2 and temperature
168 conditions for 96 hours. Pre-cultured algae were then inoculated into 500-mL
169 Erlenmeyer flasks containing 400 mL of adjusted f/2 seawater medium and
170 supplemented with 20 μmol L^{-1} KI (half saturation concentration derived from iodine
171 uptake kinetics, in Fig. S1) for 24 h. At the end of the experiment, algal samples in each
172 treatment were collected and rinsed for iodine determination within 24 h. Individual
173 flasks were cultured inside a CO_2 chamber (HP1000G-D, China), programmed to
174 supply 400 μatm, 700 μatm, 1,000 μatm, 1,500 μatm, or 2,000 μatm pCO_2 by bubbling
175 at each designated temperature for 24 h. The pH and temperature were measured at the
176 beginning and end of the experiment with a pH meter (Orion ROSS, Fisher Scientific

177 Instruments). To determine total alkalinity (TA) at each treatment, 20 ml of culture
178 medium was filtered with GF/F membrane and measured using an 848 Titrino plus
179 automatic titrator (Metrohm, Riverview, FL, USA). Chemical carbonate system
180 parameters were calculated using the CO2SYS Package in MS Excel (Pierrot, Lewis,
181 & Wallace, 2006) based on pH, temperature, salinity, and TA (Table S1).
182
183 **Potential antioxidant property of iodide in *S. japonica***
184 To determine the potential antioxidant properties of iodide in *S. japonica*,
185 oligoguluronate elicitor (GG, Shanghai Zzbio Co, Ltd, China) was used as exogenous
186 defense elicitors to induce oxidative stress and iodine efflux from algal tissue into the
187 culture medium (referred to previous study of (Küpper, Kloareg, Guern, & Potin, 2001).
188 Algal samples were inoculated into 150-mL Erlenmeyer flasks containing 100 mL
189 sterile seawater without (set as control) or with exogenous oligoguluronate elicitors at
190 a final concentration of 100 μg ml^{-1} (GG, set as treatment). Three elicitation experiments
191 were conducted at 10°C and 100 μmol photons m^{-2} s^{-1}. To understand the effect of GG
192 on iodine efflux over time, three seawater samples were randomly taken from the
193 untreated control and GG treatments at four time intervals (0 h, 1 h, 3 h, and 5 h). To
194 understand the effect of elevated pCO_2 in the presence of GG, iodine efflux was
195 measured after 3 hours under five pCO_2 conditions (400 μatm, 700 μatm, 1,000 μatm,
196 1,500 μatm, or 2,000 μatm, bubbled at 10°C for 24 h). To investigate the prolonged
197 effect of ocean acidification on iodine efflux, the short-term vs long-term response of
198 iodine efflux in *S. japonica* under ocean acidification conditions was compared. Under

short-term-ambient-carbon (SAC) and short-term-elevated-carbon (SEC) treatments, algae were pre-cultured at CO_2 concentrations of 400 μatm and 1,000 μatm respectively, for 7 days. Under long-term-ambient-carbon (LAC) or long-term-elevated-carbon (LEC) treatments, algae were pre-cultured under the same pCO_2 levels for 30 days. Following pre-culturing, iodine efflux under ambient (400 μatm) or elevated (1,000 μatm) pCO_2 was measured after 3 hours.

In situ mesocosm experiments

Three kelp species, *S. japonica*, *U. pinnatifida*, and *M. pyrifera*, as well as other coastal seaweeds (*Ulva pertusa* and *Ulva intestinalis* in Chlorophyta; *Gracilaria lemaneiformis* and *Gracilaria chouae* in Rhodophyta) were collected off the coastline of Sungo Bay for the mesocosm experiment (Fig. S2). With the exception of *M. pyrifera*, these algae are widely consumed by humans. *M. pyrifera* was selected as it is a preferred food source of marine invertebrates, such as sea urchins and abalone, which are harvested by the local fishing industry. The mesocosms were designed following (Xu et al., 2017). Six net cages (three per treatment) were used, applying two pCO_2 levels, ambient pCO_2 (400 μatm, bubbled with air) and elevated pCO_2 (1,000 μatm, bubbled with air/CO_2 premixed gas using a CO_2 Enrichlor, CE-100B; Wuhan Ruihua Instrument & 25 Equipment Ltd) (Fig. S3). One hundred and twenty individuals of each algal species of similar size were grown in each cage for approximately five months, from December 2016 to May 2017. During this period, six individuals of each algal species from each net cage (n=6) were randomly collected for iodine determination, and 10 individuals

(n=10) from each net cage were selected and weighed to monitor growth. To determine the effect of kelp size on iodine accumulation during the culture period, kelp which were pre-acclimated under ambient or elevated pCO_2 for 48 hours in the sea were sampled at different time points: 0 day, 30 days, 60 days, and 90 days for *S. japonica*, 0 day, 30 days, and 60 days for *U. pinnatifida*, and 0 day, 20 days, and 40 days for *M. pyrifera*. Seawater carbonate chemistry in the ambient (400 μatm) or elevated (1,000 μatm) pCO_2 culture environments were monitored every two days and the carbonate chemistry was calculated using the CO2SYS Package in MS Excel based on pH, temperature, salinity, and TA (Fig. S4) (for further details of the mesocosm design, see methods in supporting information).

To assess the effects of consumption of *S. japonica* by abalone, sporophytes were grown at either ambient (400 μatm) or elevated (1,000 μatm) pCO_2. Five feeding experiments were conducted *in situ*: 1) abalones were fed with ambient pCO_2-cultured *S. japonica* and were also cultured in an ambient pCO_2-cage; 2) abalones were fed with ambient pCO_2-cultured *S. japonica* and were cultured in an elevated pCO_2-cage; 3) abalones were fed with elevated pCO_2-cultured *S. japonica* and were also cultured in an elevated pCO_2-cage; 4) abalones were fed with elevated pCO_2-cultured *S. japonica* and were cultured in an ambient pCO_2-cage; 5) abalones were fed with ambient pCO_2-cultured *S. japonica* and were cultured in the sea with no cage; 6) abalones were fed with elevated pCO_2-cultured *S. japonica* and were cultured in the sea with no cage. The experiments, with six replicates (n = 6), were conducted independently for 30 days, starting on April

243 10^{th} 2017. The experimental abalones were fed with fresh algal tissue at intervals of 3
244 days and collected for iodine determination at intervals of 10 days. At the end of the
245 experiments, the abalones were cleaned with sterile seawater and the tissue was
246 removed quickly and entirely from the shell, weighed and frozen in liquid nitrogen, and
247 stored at -80 °C for total iodine and thyroid hormones (THs) determination (see
248 methods in supporting information).
249
250 **Transcriptomic and proteomic analysis of iodine metabolism in *S. japonica***
251 To explore the effect of ocean acidification on the iodine metabolism on the *S. japonica*
252 transcriptome, on day 90 of the mesocosm experiment, *S. japonica* sporophytes were
253 randomly selected, cleaned with sterile seawater, frozen in liquid nitrogen and stored at
254 -80 °C for subsequent transcriptomic (with three biological replicates for each pCO_2)
255 and proteomic (with two biological replicates for each pCO_2) analysis (see methods in
256 supporting information).
257
258 **Statistical analysis**
259 Statistical models were carried out with R software (R Core Development Team, 2014)
260 and model selection was based by Akaike Information Criterion (AIC). The effect of
261 temperature and the combined effect of increasing pCO_2 and temperature on iodine
262 accumulation were analyzed using a mixed effects model using the lmer function within
263 the package lme4 and lmerTest. When modelling the effect of temperature alone,
264 temperature was used as a fixed factor, when modelling the combined effect of

265 temperature and pCO_2, both temperature and pCO_2 were used as fixed factors (the
266 interaction between temperature and pCO_2 was dropped from the model based on AIC).
267 The effect of measurement type, either iodide or total iodine accumulation, were used
268 as random factors in both models.
269
270 Using the lm function within R, three liner models were used to compare changes in
271 iodine efflux in *S. japonica* treated with oligoguluronates (GG) or untreated (control).
272 To test for the effect of time (hours) on iodine efflux, time, treatment (GG or control),
273 and the interaction between time and treatment were included in a linear model. The
274 effect of increasing pCO_2 (400 to 2000 µatm), treatment (GG or control), and the
275 interaction between pCO_2 and treatment were included in a second linear model. The
276 effect of ambient and elevated pCO_2, treatment (GG or control), time (days), the
277 interaction between pCO_2 and time, and the interaction between treatment and pCO_2
278 were included in a third linear model.
279
280 In order to compare the responses of the three species of seaweeds used in the
281 mesocosm experiment (*S. japonica*, *M. pyrifera* and *U. pinnatifida*), the relative change
282 in iodine accumulation and weight (g) over time were calculated, relative to the
283 responses at time point zero, under control conditions (400 µatm). To test for the effect
284 of pCO_2 (ambient or elevated), over time (days), on relative changes in iodine
285 accumulation, the effect of pCO_2, time, species and the interactions between time and
286 species were included in a linear model. To test for the effect of pCO_2, over time, on

287 the relative weight of the seaweeds, the effect of pCO_2, time, species and the interaction
288 between pCO_2, time and species were included in a linear model.
289
290 Three linear models were used to test the effect of diet and pCO_2 on 1) iodine
291 enrichment 2) T3 concentration and 3) T4 concentration in the abalone *(H. discus*). For
292 iodine enrichment, the effect of diet, time, pCO_2, the interaction between diet, time and
293 pCO_2, and environment (caged or non-caged) were included in the model. For both T3
294 and T4 hormones, the effect diet, pCO_2, environment (caged or non-caged) and the
295 interaction between environment and diet were included in the model. Data collected
296 for iodine enrichment and T3 concentration best fit a lognormal distribution and for this
297 reason a generalized linear model which takes into consideration a lognormal
298 distribution was carried out, using the glm function in the stats package.
299
300 **RESULTS**
301 **Effect of increasing pCO_2 and temperature on iodine accumulation of *S. japonica***
302 **in laboratory**
303 Elevated pCO_2 caused changes in iodine accumulation in *S. japonica* when both the
304 pCO_2 and temperature were altered at the same time (Fig. 2a; $F_{1,86} = 14.515$, $P = 0.0003$),
305 with no significant effect of temperature on iodine accumulation (Fig. 2a; $F_{1,86} = 1.507$,
306 $P = 0.223$). As pCO_2 increased from 400 µatm to 1,000 µatm at the control temperature
307 (10 °C), both iodide and total iodine increased and reached the highest observed iodine
308 accumulation at 1,000 µatm. As pCO_2 increased to 1,500 µatm, iodide and total iodine

309 accumulation decreased and leveled off as pCO_2 increased to 2,000 µatm. When
310 temperature was altered in isolation, there was a significant effect on iodide and total
311 iodine accumulation in *S. japonica* (Fig. 2b; $F_{1, 27} = 19.47$, $P = 0.0002$). As temperature
312 increased, from 5 °C to 15 °C under the control pCO_2 concentration (400 µatm), iodide
313 and total iodine accumulation increased by 64% and 58%, respectively (Fig. 2b). At
314 20 °C and 23 °C, iodine accumulation decreased slightly but it was not significantly
315 different from the maximum iodine accumulation observed at 15 °C. However, there
316 were no significant effects of increasing pCO_2 or temperature (isolation or combination)
317 on iodine solubility and availability in seawater medium (Fig. S5).
318
319 **Potential antioxidant properties of iodide in *S. japonica* in laboratory**
320 Under oxidative stress, induced by the addition of oligoguluronates (GG), iodine efflux
321 in *S. japonica* was 61% greater than the untreated control group, after 5 hours (Fig. 3a;
322 $F_{1,225} = 22.428$, $P = 0.0001$). Iodine efflux in *S. japonica* treated with GG increased over
323 three hours and then decreased slightly after five hours, with little change in the
324 untreated control group over time (Fig. 3a; *effect of time on the iodine efflux,* $F_{1,47} =$
325 4.685, $P = 0.0427$) and is supported by a significant interaction between the treatment
326 (GG and control) and time (Fig. 3a; $F_{1,20} = 4.562$, $P = 0.0452$).
327
328 Iodine efflux in *S. japonica* increased with increasing pCO_2 until 1500 µatm and
329 decreased again at 2000 µatm (Fig. 3b; $F_{1,10} = 2.95$, $P = 0.098$). Iodine efflux was 51%
330 - 72% higher in *S. japonica* treated with GG than the untreated group, depending on the

331 pCO_2 levels (Fig. 3b; $F_{1,475}$ =148.375, P < 0.0001), and this is supported by a significant
332 interaction between the pCO_2 conditions and treatment (GG and untreated) (Fig. 3b;
333 $F_{1,17}$ = 5.173, P = 0.031).
334
335 Long-term exposure to elevated pCO_2 (LEC) intensified iodine efflux from *S. japonica.*
336 Iodine efflux from *S. japonica* treated with GG was 29% higher after 30 days exposure
337 to elevated pCO_2, compared with 7 days of exposure to elevated pCO_2 (SEC) and 44%
338 greater than both short- and long-term exposure to ambient pCO_2 conditions (7 days
339 and 30 days; SAC and LAC) (Fig. 3c; $F_{1,48}$ = 21.119, P = 0.0002). Very little change in
340 iodine efflux was observed in the untreated control group (Fig. 3c; $F_{1,18}$ = 107.3027, P
341 < 0.0001). This is supported by significant interactions between pCO_2 and time (Fig.
342 3c; $F_{1,12.08}$ = 5.812, P = 0.0268) and pCO_2 and treatment (GG and untreated) (Fig. 3c;
343 $F_{1,28.99}$ = 5.812, P = 0.0268).
344
345 **Effect of increasing pCO_2 on iodine accumulation of seaweeds using *in situ***
346 **mesocosm experiments**
347 In the mesocosm experiment, elevated pCO_2 increased tissue growth (relative changes
348 in fresh weight) of all three kelp species compared to ambient pCO_2 (Fig. 4 a, b and c,
349 *top panels*; $F_{1, 828}$ = 332.087, P < 0.0001). This effect was consistent over time, which
350 is supported by a significant interaction between time and pCO_2 conditions (Fig. 4 a, b
351 and c, *top panels*; $F_{1, 828}$ = 175.387, P < 0.0001). Changes in relative weight were
352 significantly different between the three species (Fig. 4 a, b and c, *top panels*; $F_{2, 828}$ =

504.273, $P < 0.0001$), including significant interactions between the species of seaweeds and time (Fig. 4 a, b and c, *top panels*; $F_{2,828} = 38.434$, $P < 0.0001$), and significant interactions between pCO_2 conditions, time and species of seaweeds (Fig. 4 a, b and c, *top panels*; $F_{2,828} = 28.354$, $P < 0.0001$). *M. pyrifera* showed the largest increase in weight under elevated pCO_2 at day 40, compared with *S. japonica* at day 90 and *U. pinnatifida* at day 60. *S. japonica* and *U. pinnatifida* showed similar changes in weight under ambient and elevated pCO_2 until day 30, thereafter *U. pinnatifida* showed larger increases in weight than *S. japonica* by day 60 (Fig. 4a).

Iodine accumulation increased in the three seaweeds under elevated pCO_2 compared to ambient pCO_2 (Fig. 4 a, b and c, *bottom panels*; $F_{1,353} = 36.362$, $P < 0.0001$). The highest iodine accumulation was observed at time zero, thereafter relative iodine accumulation declined with time (Fig. 4 a, b and c, *bottom panels*; $F_{1,353} = 791.782$, $P < 0.0001$) however, iodine accumulation declined more quickly under ambient pCO_2 conditions compared to elevated pCO_2. The three seaweeds species responded with different intensities to changes in pCO_2 (Fig. 4 a, b and c, *bottom panels*; $F_{2,353} = 16.322$, $P < 0.0001$). *S. japonica* showed the highest iodine accumulation at time zero, both under ambient pCO_2 (7.91 mg g^{-1} dw ± 0.13 SE) and elevated pCO_2 (7.87 mg g^{-1} dw ± 0.19 SE), but it also had the greatest decline in iodine accumulation over 90 days (total decline of 85% and 73% for ambient and elevated pCO_2 respectively). Compared to *S. japonica, U. pinnatifida* and *M. pyrifera* showed modest iodine accumulation at time zero. Iodine accumulation declined under both ambient and elevated pCO_2 by 58% and

375 26% respectively, over 60 days in *U. pinnatifida* (Fig. 4b) and 63% and 56%, over 40
376 days in *M. pyrifera* (Fig. 4c). This variation in iodine accumulation over time is
377 supported by a significant interaction between species of seaweeds and time (Fig. 4 a,
378 b and c, *bottom panels*; $F_{2,353} = 16.553$, $P < 0.0001$). In addition to kelp species (Fig.
379 S6), we also found similar responses to elevated pCO_2 in other seaweeds species, where
380 both algal biomass and iodine accumulation increased with the elevated pCO_2 (Fig. S7).
381
382 **Iodine transfer between *S. japonica* and its consumer *H. discus* in a mesocosm**
383 **experiment**
384 In the feeding experiment, abalone fed with *S. japonica*, cultured under elevated pCO_2
385 (1000 µatm) had a higher iodine accumulation than those fed on seaweeds cultured
386 under ambient pCO_2 (400 µatm) (Fig. 5a, $F_{1,106} = 155.24$, $P < 0.0001$). In addition,
387 iodine accumulation in the abalone was stimulated when the feeding experiments were
388 conducted under elevated pCO_2 (1000 µatm) (Fig. 5a, $F_{1,106} = 29.53$, $P < 0.0001$). Iodine
389 accumulation in all experimental abalone increased over the 30 days of cultivation (Fig.
390 5a, $F_{1,105} = 1003.48$, $P < 0.0001$), and abalone fed with seaweeds grown under high pCO_2
391 and under elevated pCO_2 conditions showed the highest amount of iodine accumulation
392 (Fig. 5a; *interaction between diet, time and* pCO_2, $F_{1,102} = 26.29$, $P < 0.0001$). There
393 was no difference in iodine accumulation between feeding experiments conducted in a
394 cage or in the field with no cage (Fig. 5a, $F_{1,103} = 1.31$, $P = 0.255$).
395
396 It was found that both T3 (Fig. 5b; $F_{1,33} = 831.98$, $P < 0.0001$) and T4 (Fig. 5b; $F_{1,33} =$

482.77, $P < 0.0001$) hormone concentrations declined when the abalone were fed with *S. japonica* cultured under elevated pCO_2, regardless of the pCO_2 conditions of the feeding experiment. Whilst there was a decline in thyroid concentration under elevated pCO_2, for both T3 (Fig. 5b; $F_{1,34} = 143.29$, $P < 0.0001$) and T4 concentrations ($F_{1,34} = 183.36$, $P < 0.0001$), the largest drop in thyroid concentration occurred when abalone were fed with algae cultured under high pCO_2 and under elevated pCO_2 conditions. Linear regression analysis further demonstrated that dietary inclusion of *S. jap*onica with higher iodine content caused an increase in iodine intake into the abalone (Fig. S8a) and resulted in lower concentration of T3 (Fig. S8b) and T4 (Fig. S8c) hormones. Moreover, results also revealed that there were significant negative relationships between iodine concentration and T3 (Fig. S9a) and T4 content (Fig. S9b). Overall, THs concentrations were higher in the field with no cage for both T3 (Fig. 5b; $F_{1,32} = 324.30$, $P < 0.0001$) and T4 (Fig. 5b; $F_{1,32} = 284.49$, $P < 0.0001$) hormones. However, THs concentration drop in field conditions when abalone were fed with algae cultured under elevated pCO_2, and this is supported by a significant interaction between the pCO_2 level that dietary seaweeds were cultured under and the conditions of the feeding experiment (i.e. caged or not caged), for both T3 concentrations (Fig. 5b; $F_{1,31} = 23.93$, $P < 0.0001$) and T4 concentrations (Fig. 5b; $F_{1,31} = 47.16$, $P < 0.0001$).

In situ transcriptional or proteomic response of _S. japonica_ to elevated pCO_2

Transcriptome data showed that 11 *vIPO* (vanadium-dependent iodoperoxidases) and 12 *vBPO* (vanadium-dependent bromoperoxidases) UniGenes were significantly

differentially expressed between ambient and elevated pCO_2 of culture environments (Fig. 6a). Among these genes, 8 *vIPOs* and 8 *vBPOs* were down-regulated, whereas 3 *vIPOs* and 4 *vBPOs* were up-regulated under elevated pCO_2 in the mesocosms (Table S2, S3). The variation trend was verified for 8 genes by RT-PCR (Fig. S10). In the proteomic data, it was found that four vHPOs proteins were down-regulated at elevated pCO_2 (Fig. 6b). Therein, the trend of relative expression of two vBPOs (SJ19768 and SJ19850) was consistent with those in the transcriptome. In contrast, vIPOs (SJ00628) and vBPOs (SJ10798) did not significantly change at the transcriptomic level.

DISCUSSION

Brown algae are predicted to benefit from elevated pCO_2 under global change (Enochs et al., 2015; Johnson, Russell, Fabricius, Brownlee, & Hall-Spencer, 2012; Linares et al., 2015; Porzio, Buia, & Hall-Spencer, 2011; Xu et al., 2017) and therefore will thrive in natural pCO_2 rich environments (Enochs et al., 2015; Johnson, Russell, Fabricius, Brownlee, & Hall-Spencer, 2012; Linares et al., 2015; Porzio, Buia, & Hall-Spencer, 2011). It is supported by data that tissue growth of *S. japonica* (Fig. 2 and Fig. 4a), *U. pinnatifida* (Fig. 4b), and *M. pyrifera* (Fig. 4c), and photosynthesis of *S. japonica* (Fig. S11) all increased under elevated CO_2 conditions. However, it was unknown how enhanced growth of kelp, under conditions of ocean acidification, affect the accumulation and transfer of iodine across coastal marine foodwebs. Increasing pCO_2 will not change the solubility and availability of inorganic iodine in seawater (Fig. S5). However, the data presented here reveal for the first time that increasing pCO_2 causes

441 iodine accumulation in coastal seaweeds and leads to the accumulation of iodine in
442 consumers of kelp, which potentially will result in elevated iodine intake of consumers
443 of kelp if pCO_2 continues to rise (1,000 µatm in 2100 under RCP 8.5) as predicted by
444 climate models (Fig. 1).
445
446 In laboratory experiment, we found that at pCO_2 greater than 400 µatm (the current
447 pCO_2 value), changes in temperature had no effect on iodine accumulation and
448 predictions of iodine accumulation in *S. japonica* could be made based on changes in
449 pCO_2 alone (Fig. 2). It is suggested that this is because pCO_2 is the dominant
450 environmental driver when pCO_2 and temperature change simultaneously. This finding
451 is supported by Brennan and Collins (2015) who demonstrated that changes in the
452 growth rate of the microalgae *Chlamydomonas reinhardtii* could be predicted using the
453 dominant environmental driver in test environments with up to eight environmental
454 drivers (Brennan & Collins, 2015). Global change will involve many simultaneous
455 environmental changes, such as changes in CO_2, pH, temperature, and nutrient (Boyd,
456 Lennartz, Glover, & Doney, 2015; Gruber, 2011; Hutchins & Fu, 2017). Results
457 presented here highlight the importance of measuring the response to multiple
458 environmental drivers in order to understand how they interact. Predictions on the
459 combined effects of environmental drivers using traditional additive or multiplicative
460 models could potentially overestimate the effects of ocean warming and ocean
461 acidification on iodine accumulation (Fig. S12).
462

463 Elevated iodine accumulation in *S. japonica* under ocean acidification was associated
464 with down-expression regulation of vHPOs (vIPOs and vBPOs), which has never been
465 observed before in any alga (Fig. 6). While vHPOs specific physiological role is still
466 unclear, these genes have previously been studied for their role in the oxidative stress
467 response in brown algae including, *S. japonica* (Ye et al., 2015) and *Laminaria digitata*
468 (Cosse et al., 2009). In addition, the physiological antioxidant role of iodine in algae is
469 suggested to be linked to the presence of particular *vHPO*s (Colin et al., 2003, 2005).
470 Under oxidative stress, induced by elicitor-triggered oxidative burst, iodine efflux
471 increased in *S. japonica*, even under high pCO_2 (Fig. 3), supporting the physiological
472 role of iodine in algae. In some cases, the iodine efflux was up to twice as high as in the
473 control group (Fig. 3a). Thus, iodine efflux is probably an efficient strategy to cope with
474 oxidative stress (Küpper et al., 2008). Furthermore, the oligoalginate-triggered
475 oxidative burst and associated iodide release is also known to be an efficient strategy
476 against infection, suggesting that under ocean acidification kelp may be able to cope
477 better with infections as they have more stored iodine (Küpper et al., 2008; Küpper,
478 Müller, Peters, Kloareg, & Potin, 2002).
479
480 Elevated iodine content in kelp has the potential to be transferred to their consumers
481 such as abalone. *H. discus* fed with algae cultured under elevated CO_2 showed higher
482 levels of iodine accumulations and reduced levels of T3 and T4 hormones compared to
483 animals fed with algae cultured under ambient CO_2 (Fig. 5). Iodine is essential for the
484 synthesis of thyroid hormones (THs), which play important roles in development,

485 metamorphosis and metabolism of vertebrates and invertebrates, including humans
486 (Bath et al., 2017; Huang et al., 2015). Previous studies have demonstrated that sea
487 urchin larvae could potentially receive TH precursors or the active hormones from some
488 of the microalgal species that they consumed (Heyland & Moroz, 2006). Whilst, few
489 data were available on the effect of iodine intake on the THs of invertebrates, some
490 studies on humans demonstrate that high-dose kelp supplementation significantly
491 decreased the total triiodothyronine levels of subjects (Eliason, 1998). The increased
492 iodine transfer and reduced thyroid hormones could potentially impact nutrient
493 composition of costal primary producers as well as in kelp-based coastal food webs.
494
495 Our results suggest that projected pCO_2 (1,000 µatm in 2100 under RCP 8.5) will
496 increase the growth of coastal seaweeds and their iodine accumulation, with the
497 potential for higher levels of iodine to be transferred from seaweeds to consumers. Thus,
498 there is a potential risk of iodine overconsumption in consumers of kelps if pCO_2
499 increases as projected for the coming decades. Furthermore, biogeochemical cycling of
500 iodine in coastal ecosystems might change as a consequence of enhanced accumulation
501 in coastal marine foodwebs. This may even have consequences for coastal non-marine
502 habitats as volatile iodinated compounds can be released to the atmosphere (Cosse,
503 Potin, & Leblanc, 2009; Küpper & Kroneck, 2014).
504
505 **ACKNOWLEDGEMENTS**
506 We thank F. Weinberger and P. Kroth for revision of the manuscript. This work was

supported by National Natural Science Foundation of China (41676145); Shandong key Research and Development Plan (2018GHY115010); Central Public-interest Scientific Institution Basal Research Fund CAFS (2017HY-YJ01); Qingdao Municipal Science and Technology plan project (17-1-1-96-jch); Special Scientific Research Funds for Central Non-Profit Institutes, Yellow Sea Fisheries Research Institute, Chinese Academy of Fishery Sciences (20603022016010, 20603022016001); China Agriculture Research System (CARS-50); Taishan Scholars Funding; AoShan Talents Program (No. 2015ASTPES03); the Science Fund for Distinguished Young Scholars of Shandong Province (JQ201509).

REFERENCES

Bath, S. C., Hill, S., Infante, H. G., Elghul, S., Nezianya, C. J., & Rayman, M. P. (2017). Iodine concentration of milk-alternative drinks available in the UK in comparison with cows' milk. *British Journal of Nutrition*, *118*, 525–532.

Berg, V., Nøst, T. H., Skeie, G., Thomassen, Y., Berlinger, B., Veyhe, A. S., … Hansen, S. (2017). Thyroid homeostasis in mother–child pairs in relation to maternal iodine status: the MISA study. *European Journal of Clinical Nutrition*, *71*, 1002–1007.

Bloom, A. J., Burger, M., Asensio, J. S. R., & Cousins, A. B. (2010). Carbon dioxide enrichment inhibits nitrate assimilation in wheat and *Arabidopsis*. *Science*, *328*, 899–903.

Boyd, P. W., Lennartz, S. T., Glover, D. M., & Doney, S. C. (2015). Biological ramifications of climate-change-mediated oceanic multi-stressors. *Nature Climate*

529 *Change*, *5*, 71.
530 Brennan, G., & Collins, S. (2015). Growth responses of a green alga to multiple
531 environmental drivers. *Nature Climate Change*, *5*, 892.
532 Butler, A., & Carter-Franklin, J. N. (2004). The role of vanadium bromoperoxidase in
533 the biosynthesis of halogenated marine natural products. *Natural Product Reports*,
534 *21*, 180–188.
535 Colin, C., Leblanc, C., Michel, G., Wagner, E., Leize-Wagner, E., Van Dorsselaer, A.,
536 & Potin, P. (2005). Vanadium-dependent iodoperoxidases in *Laminaria digitata*, a
537 novel biochemical function diverging from brown algal bromoperoxidases. *JBIC*
538 *Journal of Biological Inorganic Chemistry*, *10*, 156–166.
539 Colin, C., Leblanc, C., Wagner, E., Delage, L., Leize-Wagner, E., Van Dorsselaer, A., ...
540 & Potin, P. (2003). The brown algal kelp *Laminaria digitata* features distinct
541 bromoperoxidase and iodoperoxidase activities. *Journal of Biological Chemistry*,
542 *278*, 23545.
543 Cosse, A., Potin, P., & Leblanc, C. (2009). Patterns of gene expression induced by
544 oligoguluronates reveal conserved and environment-specific molecular defense
545 responses in the brown alga *Laminaria digitata*. *New Phytologist*, *182*, 239–250.
546 Dillon, M. E., Wang, G., & Huey, R. B. (2010). Global metabolic impacts of recent
547 climate warming. *Nature*, *467*, 704.
548 Eliason, B. C. (1998). Transient hyperthyroidism in a patient taking dietary
549 supplements containing kelp. *The Journal of the American Board of Family*
550 *Practice*, *11*, 478–480.

551 Enochs, I. C., Manzello, D. P., Donham, E. M., Kolodziej, G., Okano, R., Johnston,
552 L., ... & Valentino, L. (2015). Shift from coral to macroalgae dominance on a
553 volcanically acidified reef. *Nature Climate Change*, *5*, 1083.
554 Gruber, N. (2011). Warming up, turning sour, losing breath: ocean biogeochemistry
555 under global change. *Philosophical Transactions of the Royal Society of London*
556 *A: Mathematical, Physical and Engineering Sciences*, *369*, 1980–1996.
557 Guillard, R. R. L. (1975). Culture of phytoplankton for feeding marine invertebrates.
558 In W. L. Smith & M. H. Chanley (Eds.), *Culture of marine invertebrate animals*
559 (pp. 26–60). New York, NY: Plenum Press.
560 Heyland, A., & Moroz, L. L. (2006). Signaling mechanisms underlying metamorphic
561 transitions in animals. *Integrative and Comparative Biology*, *46*, 743–759.
562 Huang, W., Xu, F., Qu, T., Zhang, R., Li, L., Que, H., & Zhang, G. (2015). Identification
563 of thyroid hormones and functional characterization of thyroid hormone receptor
564 in the pacific oyster *Crassostrea gigas* provide insight into evolution of the thyroid
565 hormone system. *PloS One*, *10*, e0144991.
566 Hutchins, D. A., & Fu, F. (2017). Microorganisms and ocean global change. *Nature*
567 *Microbiology*, *2*, 17058.
568 Jin, P., Wang, T., Liu, N., Dupont, S., Beardall, J., Boyd, P. W., ... & Gao, K. (2015).
569 Ocean acidification increases the accumulation of toxic phenolic compounds
570 across trophic levels. *Nature Communications*, *6*, 8714.
571 Johnson, V. R., Russell, B. D., Fabricius, K. E., Brownlee, C., & Hall-Spencer, J. M.
572 (2012). Temperate and tropical brown macroalgae thrive, despite decalcification,

along natural CO_2 gradients. *Global Change Biology*, *18*, 2792–2803.

Küpper, F. C. (2015). Iodine in Seaweeds–Two Centuries of Research. In Springer Handbook of Marine Biotechnology (pp. 591-596). Springer, Berlin, Heidelberg.

Küpper, F. C., & Kroneck, P. M. (2014). Iodine bioinorganic chemistry: physiology, structures, and mechanisms. *Iodine Chemistry and Applications*, 555–589.

Küpper, F. C., Carpenter, L. J., McFiggans, G. B., Palmer, C. J., Waite, T. J., Boneberg, E. M., ... & Potin, P. (2008). Iodide accumulation provides kelp with an inorganic antioxidant impacting atmospheric chemistry. *Proceedings of the National Academy of Sciences*, *105*, 6954–6958.

Küpper, F. C., Kloareg, B., Guern, J., & Potin, P. (2001). Oligoguluronates elicit an oxidative burst in the brown algal kelp *Laminaria digitata*. *Plant Physiology*, 125, 278–291.

Küpper, F. C., Müller, D. G., Peters, A. F., Kloareg, B., & Potin, P. (2002). Oligoalginate recognition and oxidative burst play a key role in natural and induced resistance of sporophytes of Laminariales. *Journal of Chemical Ecology*, *28*, 2057–2081.

Leung, A. M., & Braverman, L. E. (2014). Consequences of excess iodine. *Nature Reviews Endocrinology*, *10*, 136.

Linares, C., Vidal, M., Canals, M., Kersting, D. K., Amblas, D., Aspillaga, E., ... & Hereu, B. (2015). Persistent natural acidification drives major distribution shifts in marine benthic ecosystems. *Proc. R. Soc. B*, *282*, 20150587.

Loladze, I. (2002). Rising atmospheric CO_2 and human nutrition: toward globally imbalanced plant stoichiometry?. *Trends in Ecology & Evolution*, *17*, 457–461.

595 Martínez-Botí, M. A., Foster, G. L., Chalk, T. B., Rohling, E. J., Sexton, P. F., Lunt, D.
596 J., ... & Schmidt, D. N. (2015). Plio-Pleistocene climate sensitivity evaluated using
597 high-resolution CO_2 records. *Nature*, *518*, 49.
598 McKibben, S. M., Peterson, W., Wood, A. M., Trainer, V. L., Hunter, M., & White, A.
599 E. (2017). Climatic regulation of the neurotoxin domoic acid. *Proceedings of the*
600 *National Academy of Sciences*, *114*, 239–244.
601 Myers, S. S., Smith, M. R., Guth, S., Golden, C. D., Vaitla, B., Mueller, N. D., ... &
602 Huybers, P. (2017). Climate change and global food systems: potential impacts on
603 food security and undernutrition. *Annual Review of Public Health*, *38*, 259–277.
604 Nitschke, U., & Stengel, D. B. (2015). A new HPLC method for the detection of iodine
605 applied to natural samples of edible seaweeds and commercial seaweed food
606 products. *Food Chemistry*, *172*, 326–334.
607 Phalkey, R. K., Aranda-Jan, C., Marx, S., Höfle, B., & Sauerborn, R. (2015). Systematic
608 review of current efforts to quantify the impacts of climate change on
609 undernutrition. *Proceedings of the National Academy of Sciences*, *112*, 4522–4529.
610 Pierrot, D. E., Lewis, E., & Wallace, D. W. R. (2006). MS Excel program developed for
611 CO_2 system calculations. Oak Ridge, TN: Carbon Dioxide Information Analysis
612 Center, Oak Ridge National Laboratory, U.S. Department of Energy. doi:
613 10.3334/CDIAC/otg.CO2SYS_XLS_CDIAC105a
614 Porzio, L., Buia, M. C., & Hall-Spencer, J. M. (2011). Effects of ocean acidification on
615 macroalgal communities. *Journal of Experimental Marine Biology and Ecology*,
616 *400*, 278–287.

617 R Core Development Team. (2014). R: A language and environment for statistical
618 computing: R Foundation for Statistical Computing. http://www.R-project.org/.
619 Strittmatter, M., Grenville-Briggs, L. J., Breithut, L., Van West, P., Gachon, C. M., &
620 Küpper, F. C. (2016). Infection of the brown alga *Ectocarpus siliculosus* by the
621 oomycete *Eurychasma dicksonii* induces oxidative stress and halogen metabolism.
622 *Plant Cell & Environment*, *39*, 259–271.
623 Sunday, J. M., Fabricius, K. E., Kroeker, K. J., Anderson, K. M., Brown, N. E., Barry,
624 J. P., ... & Klinger, T. (2017). Ocean acidification can mediate biodiversity shifts
625 by changing biogenic habitat. *Nature Climate Change*, *7*, 81.
626 Thomsen, J., Stapp, L. S., Haynert, K., Schade, H., Danelli, M., Lannig, G., ... &
627 Melzner, F. (2017). Naturally acidified habitat selects for ocean acidification–
628 tolerant mussels. *Science Advances*, *3*, e1602411.
629 Ullah, H., Nagelkerken, I., Goldenberg, S. U., & Fordham, D. A. (2018). Climate
630 change could drive marine food web collapse through altered trophic flows and
631 cyanobacterial proliferation. *PLoS Biology*, *16*, e2003446.
632 Xu, D., Schaum, C. E., Lin, F., Sun, K., Munroe, J. R., Zhang, X. W., ... & Ye, N. (2017).
633 Acclimation of bloom-forming and perennial seaweeds to elevated pCO_2
634 conserved across levels of environmental complexity. *Global Change Biology*, *23*,
635 4828–4839.
636 Ye, N., Zhang, X., Miao, M., Fan, X., Zheng, Y., Xu, D., ... & Wang, Y. (2015).
637 *Saccharina* genomes provide novel insight into kelp biology. *Nature*
638 *Communications*, *6*, 6986.

Zhang, K., Song, C., Zhang, Y., Dang, H., Cheng, X., & Zhang, Q. (2018). Global-scale patterns of nutrient density and partitioning in forests in relation to climate. *Global Change Biology*, *24*, 536–551.

Zhu, C., Kobayashi, K., Loladze, I., Zhu, J., Jiang, Q., Xu, X., ... & Fukagawa, N. K. (2018). Carbon dioxide (CO_2) levels this century will alter the protein, micronutrients, and vitamin content of rice grains with potential health consequences for the poorest rice-dependent countries. *Science Advances*, *4*, eaaq1012.

SUPPORTING INFORMATION

Additional Supporting Information may be found in the online version of this article:

Table S1. Carbonate system data (mean ± standard errors) in the laboratory set up using the CO2SYS Package.

Table S2. The genes used for real-time quantitative PCR (RT-qPCR) *S. japonica* cultured in field experiment under ambient (bubbled with air) and elevated pCO_2 (bubbled with mix air of 1,000 μatm CO_2).

Table S3. The primers used for real-time quantitative PCR (RT-qPCR) of *S. japonica* cultured in field experiment under ambient (bubbled with air) and elevated pCO_2 (bubbled with mix air of 1,000 μatm CO_2).

Fig. S1. Kinetics of iodine influx by *S. japonica* sporophyte under of various concentrations of KI. (a) Iodine influx rate (IIR) of *S. japonica* sporophyte. (b) The Lineweaver-Burk plots between KI substrate and iodine influx rate which was used for

Lineweaver-Burk K_m and IUR_{max} determination. In a laboratory set up, kinetics of iodine influx of *S. japonica* under a series of iodide concentration in surrounding medium were determined over a duration of 24 hours. With increasing concentration of iodide (1-30 μmol L^{-1} KI), the influx rate increased significantly until the external KI concentration exceeded 10 μmol L^{-1} (One-Way ANOVA, df=5, $P<0.001$). Furthermore, iodine influx followed a Michaelis-Menten equation and Lineweaver-Burk plot was used for $K_{1/2}$ (19.94 μmol L^{-1}) and IIR_{max} (15.04 μmol g^{-1} dry weight h^{-1}) determination ($R^2=0.9547$, df=1, F=84.229, $P<0.05$).

Fig. S2. Experimental design of the field experiment. pCO_2 treatments were carried out in triplicate tanks (n=3 per pCO_2 level), under ambient pCO_2 (400 μatm, bubbled with air) and elevated pCO_2 (bubbled with air/CO_2 premixed gas using a CO_2 Enrichlor). In the field experiment, we held all seaweed species simultaneously as logistics did not allow for each species to be grown on its own at each pCO_2 level at sufficient replication. The letters in the net cages represent experimental algal species used in the mesocosms including *S. japonica* (a), *U. pinnatifida* (b), *M. pyrifera* (c), *G. lemaneifor* (d), *G. chouae* (e), *U. pertusa* (f), and *U. intestinalis* (g).

Fig. S3. Example for coastal mesocosms on the sea. (a) photograph of net cages and CO_2 Enrichlor used for ocean acidification experiment; (b) Variation of nutrient (mean ± standard errors, n=6); (c) Variation in temperature; (d) Variation of irradiance. During the culture period (160 days), the seawater temperature initially decreased from 10.36 ± 0.44 °C to 2.08 ± 0.17 °C after 80 days and then increased from 2.37 ± 0.48 °C to 12.73 ± 0.22 °C. The average irradiance was 98 μmol photons m^{-2} s^{-1} and the light

683 condition would not limit algal growth.

684 **Fig. S4. Variation of seawater carbonate chemistry (mean ± standard error) under**
685 **low (400 µatm bubbled with air) or high pCO_2 (1,000 µatm bubbled with air/CO_2**
686 **premixed gas using a CO_2 Enrichlor) conditions for more than 5 months in the**
687 **coastal field experiment.** (a) pH; (b) Total alkalinity (TA); (c) DIC; (d)HCO_3^-; (e)
688 CO_3^{2-}; (f) CO_2. The shaded areas indicate the standard deviation of three replicates.

689 **Fig. S5. The individual and combined effect of increasing pCO_2 and temperature**
690 **on iodine solubility and availability.** Colored columns show the observed variation of
691 iodide (a) or iodate (b) concentration of three biological replicates (± SE) under
692 increasing pCO_2 at different temperatures of 5°C, 10°C, 15°C, 20°C and 25°C.

693 **Fig. S6. Algal fresh weight (top panels) and iodine accumulation (bottom panels)**
694 **under ambient pCO_2 (400 µatm, bubbled with air, blue) and elevated pCO_2**
695 **(bubbled with mix air of 1,000 µatm CO_2, red) for (a) *S. japonica*, (b) *U. pinnatifida*,**
696 **and (c) *M. pyrifera* in mesocosm experiments.** Colored circles show the average of
697 biological replicates at each time point (± SE), with n=30 for fresh weight and n=18 for
698 iodine accumulation.

699 **Fig. S7. Algal fresh weight (top panels) and iodine accumulation (bottom panels)**
700 **under ambient pCO_2 (400 µatm, bubbled with air, blue) and elevated pCO_2**
701 **(bubbled with mix air of 1,000 µatm CO_2, red) for (a) *U. pertusa*, (b) *U. intestinalis*,**
702 **(c) *G. lemaneiformis*, and (d) *G. chouae* in mesocosm experiment.** Colored circles
703 show the average of biological replicates at each time (± SE), with n=30 for fresh weight
704 and n=18 for iodine accumulation.

Fig. S8. Linear regression analysis between the iodine concentration of *S. japonica* and iodine concentration or THs synthesis in the consumer *H. discus*. (a) Linear regression analysis between the iodine concentration in *S. japonica* and iodine concentration in *H. discus*; (b) Linear regression analysis between the iodine concentration in *S. japonica* and T3 concentration in *H. discus*; (c) Linear regression analysis between the iodine concentration in *S. japonica* and T4 concentration in *H. discus*.

Fig. S9. Linear regression analysis between the iodine concentration and THs synthesis in *H. discus*. (a) Linear regression analysis between the iodine concentration and T3 concentration; (b) Linear regression analysis between the iodine concentration and T4 concentration.

Fig. S10. Relative expression level of several *vHPO* genes by real-time quantitative PCR (RT-qPCR).

Fig. S11. The individual and combined effects of temperature and pCO_2 on F_v/F_m of *S. japonica* in laboratory set up. (a) The individual effect of increasing temperature on F_v/F_m where culture pCO_2 was set at 400 μatm and bubbled with air; (b) The individual effect of increasing pCO_2 on F_v/F_m where the temperature was maintained at 10 °C; (c) The combined effects of high temperature of 15 °C and increasing pCO_2 on F_v/F_m; (d) The combined effects of high temperature of 20 °C and increasing pCO_2 on F_v/F_m.

Fig. S12. Comparing the observed effect and the predicted effect of increasing pCO_2 and temperature on the kelp *S. japonica*. Filled circles show the

observed response in total iodine accumulation of three biological replicates (± SE) under increasing pCO_2 at different temperatures; 10°C (grey), 15°C (yellow) and 20°C (blue). Colored solid lines show the predicted response of iodine accumulation under increasing pCO_2 at different temperatures; 15°C (yellow) and 20°C (blue) using (a) the additive model and (b) the multiplicative model. The dashed grey line shows the observed response of increasing pCO_2 under control temperature conditions (10°C). This is equivalent to predictions based on the dominant environmental driver (in this example the dominant driver is pCO_2) and demonstrates that predictions on iodine accumulation in *S. japonica* are most accurate when based on the response to pCO_2 alone. Note that the y-axis differ between panels a and b.

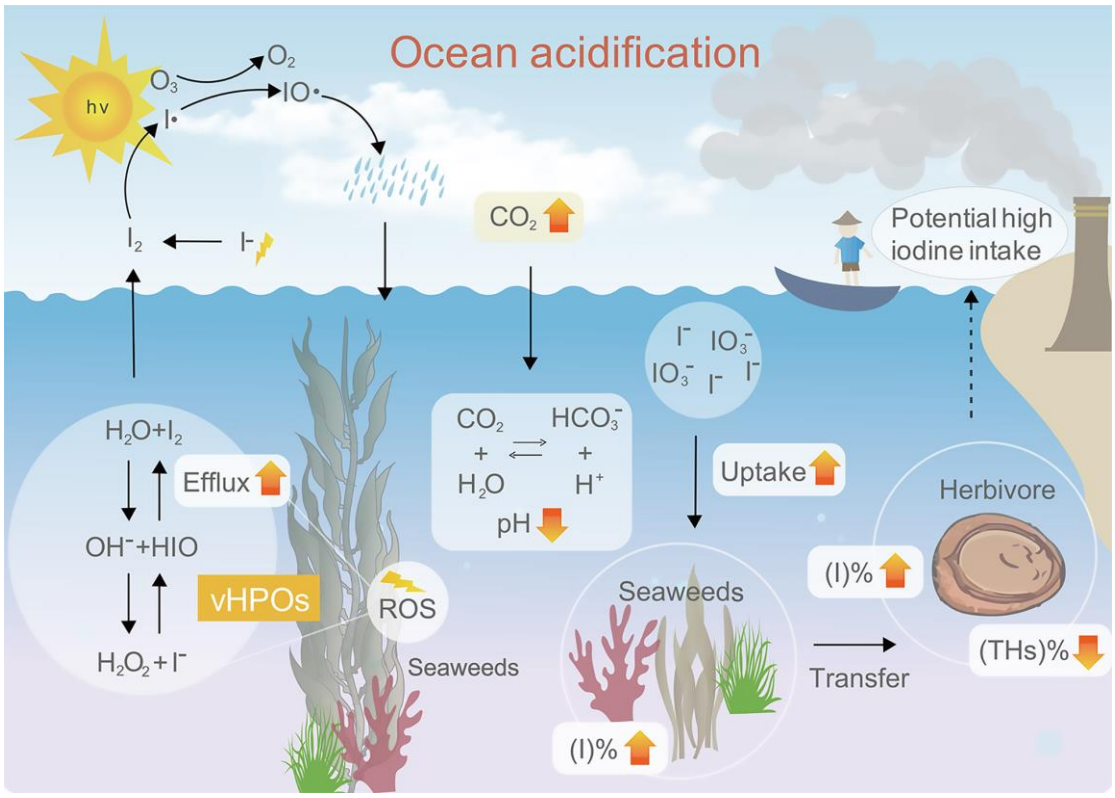

738

739 **Fig. 1. Conceptual diagram showing altered iodine metabolic pathway and global**

740 **iodine geochemical cycle under ocean acidification.** The yellow up arrows indicate

741 the up-regulated pathway; the yellow down arrows indicate the down-regulated

742 pathway; the black arrow with dashed lines indicates the possible outcome under further

743 ocean acidification. The abbreviations ROS represents the reactive oxygen species;

744 vHPOs represents the vanadium-dependent haloperoxidases; THs represents the

745 thyroid hormones.

746

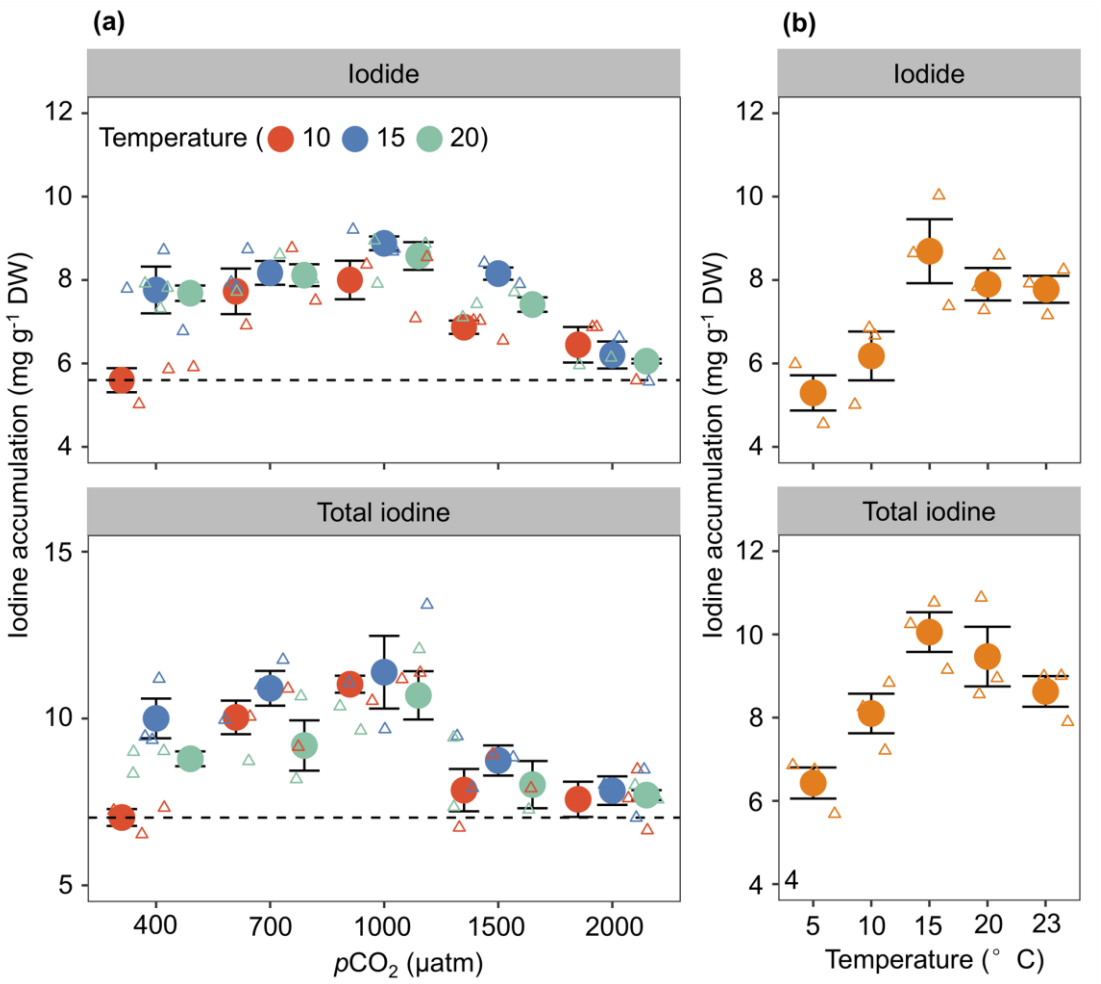

Fig. 2. The combined effect of increasing pCO_2 and temperature and the effect of increasing temperature alone on iodine accumulation in the kelp *S. japonica*. Filled circles show the average iodide (top panels) and total iodine (bottom panels) accumulation in three biological replicates (± SE). (a) Colored circles show the combined effects of increasing pCO_2 at different temperatures; 10°C (red), 15°C (blue) and 20°C (green). Horizontal dashed lines indicate the iodine accumulation under control temperature (10°C) and pCO_2 (400 µatm) conditions. (b) Colored circles (orange) show that iodide and total iodine accumulation increases with increasing temperature under control pCO_2 levels (400 µatm).

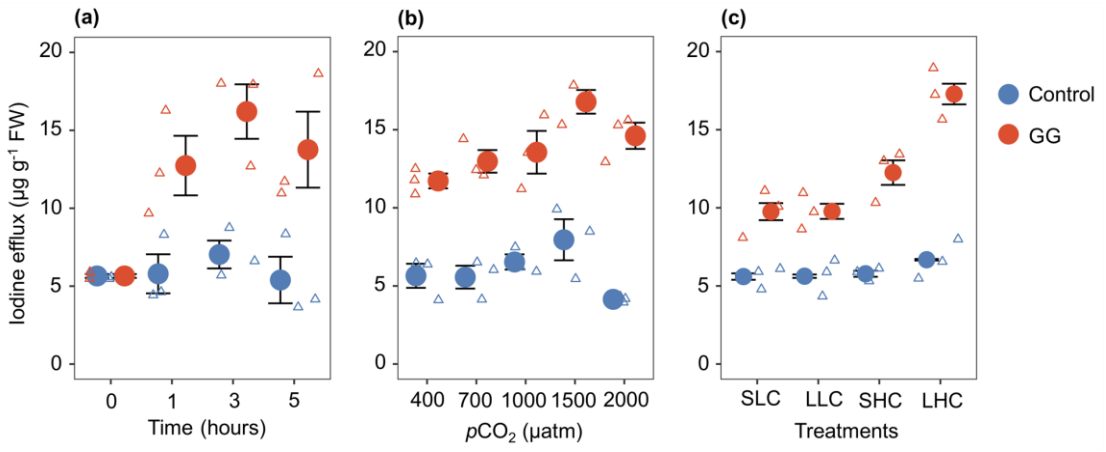

758

759 **Fig. 3. The effect of increasing pCO_2 on iodine efflux of *S. japonica* upon**
760 **oligoguluronate-triggered oxidative burst in laboratory experiment.** Colored
761 circles show the average iodine efflux of three biological replicates (± SE) under
762 oligoguluronate elicitor (GG, blue) and Control (red) conditions. (a) The change in
763 iodine efflux of *S. japonica* under GG and control conditions over 5 hours at 10°C ; (b)
764 The effect of increasing pCO_2 on iodine efflux of *S. japonica* after 3 hours of GG
765 elicitation at 10°C; (c) The short-term elevated pCO_2 vs long-term elevated pCO_2 effect
766 on iodine efflux 10°C. Treatments shown in the x-axis denote the culture conditions of
767 *S. japonica*; SAC = short-term (7 days) under ambient carbon (400 µatm), SEC = short-
768 term (7 days) under elevated-carbon (1,000 µatm), LAC = long-term (30 days) under
769 ambient-carbon (400 µatm), and LEC = long-term (30 days) under elevated-carbon
770 (1,000 µatm).

771

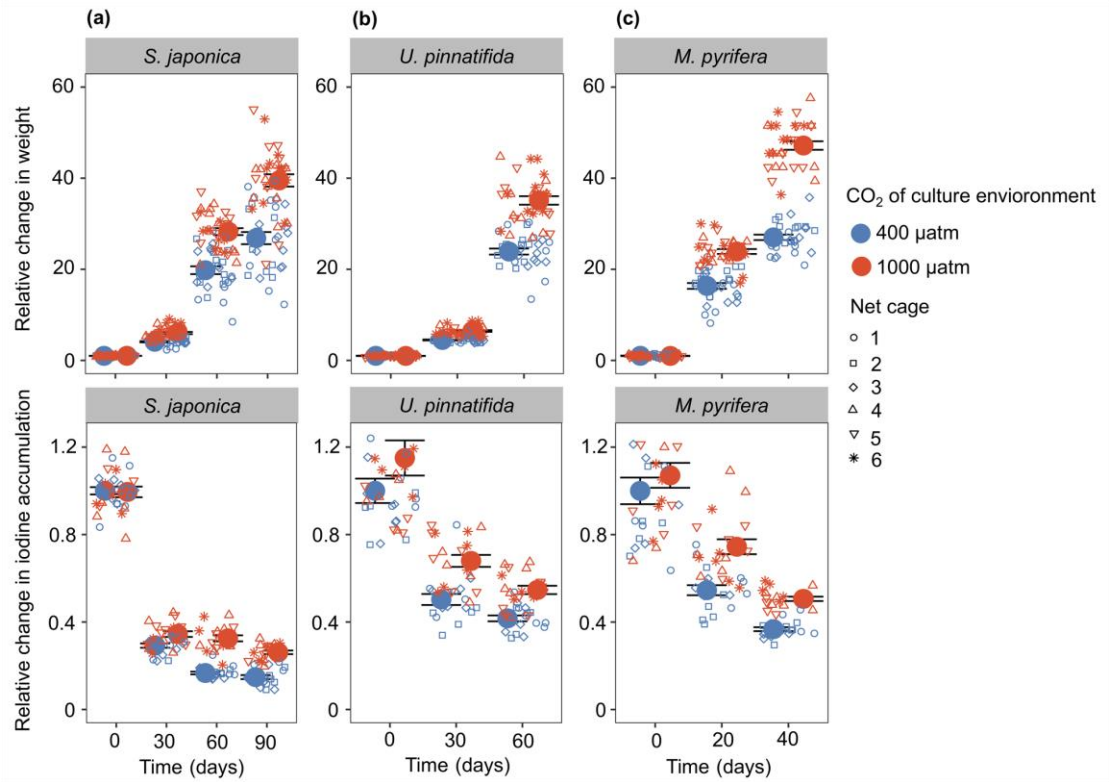

772

773 **Fig. 4. Relative changes in weight (top panels) and relative changes in iodine**

774 **accumulation (bottom panels) under ambient *p*CO2 (400 µatm, bubbled with air,**

775 **blue) and elevated *p*CO2 (bubbled with mix air of 1,000 µatm CO2, red), in a**

776 **mesocosm experiment.** Three kelp species (a) *S. japonica*, (b) *U. pinnatifida*, (c) *M.*

777 *pyrifera* were cultured in mesocosm experiment. Colored circles show the average of

778 biological replicates at each time (± SE), with n=30 for the relative changes in weight

779 and n=18 for the relative changes in iodine.

780

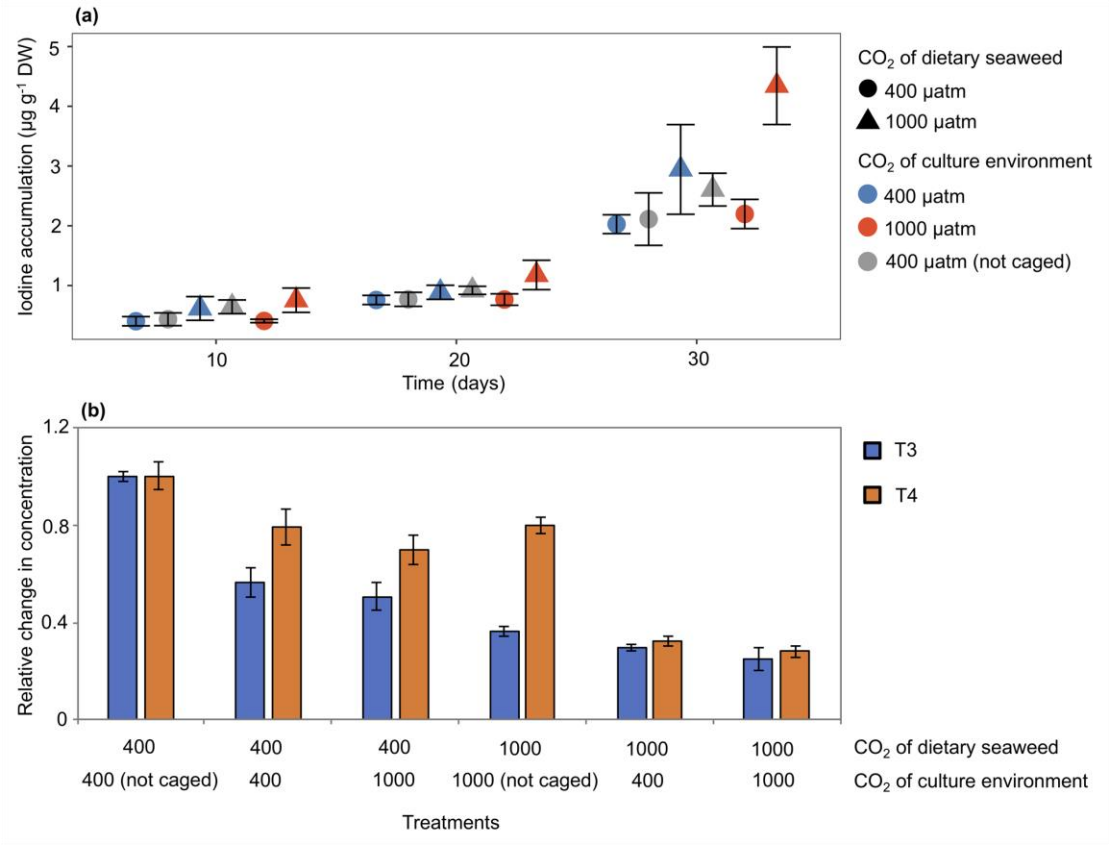

781

782 **Fig. 5. Changes in iodine accumulation and thyroid hormones (THs) synthesis in**

783 ***H. discus* fed with seaweeds cultured under either ambient and elevated pCO_2.**

784 Colored symbols show the average iodine accumulation of six biological replicates (±

785 SE) fed with either *S. japonica* cultured under 400 μatm (circles) or 1,000 μatm

786 (triangles) pCO_2. Feeding trials were conducted inside a cage under either 1,000 μatm

787 (red symbols) or 400 μatm (blue symbols) pCO_2 or in the field with no cage under 400

788 μatm (gray symbols) pCO_2. (a) Changes in iodine accumulation in *H. discus* were

789 measured every 10 days for 30 days. (b) Changes in the concentrations of

790 triiodothyronine (T3) and thyroxine (T4) at day 30, relative to data collected from

791 feeding experiments with algae cultured under 400 μatm, in the field.

792

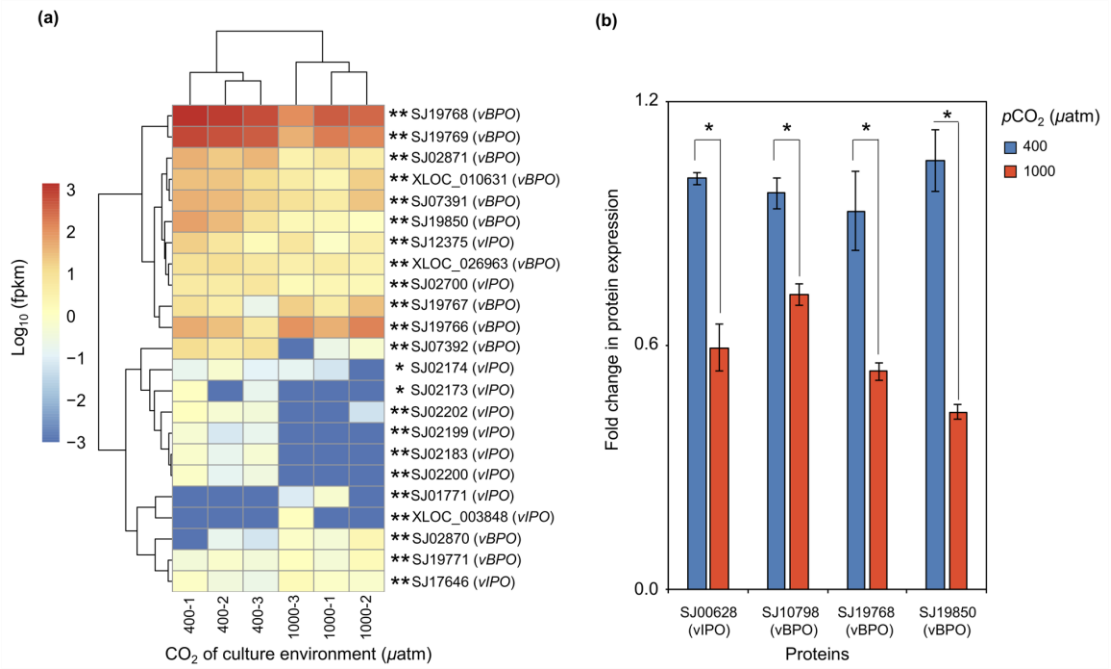

793

794 **Fig. 6. The effect of increasing pCO_2 on the relative expression of vHPO at**

795 **transcriptomic or proteomic level in *S. japonica* cultured under ambient (400 µatm)**

796 **or elevated (1,000 µatm) pCO_2 scenarios, using an *in situ* mesocosm experiment.**

797 (a) Variation of *vHPO* gene expression; (b) Variation of vHPO protein expression. * (p-

798 value <0.05) and ** (p-value <0.001) represent significant differences between

799 treatments of ambient (400 µatm) or high (1,000 µatm) pCO_2.